

See discussions, stats, and author profiles for this publication at: <https://www.researchgate.net/publication/231633343>

Benzopinacol Radical Cation

ARTICLE *in* THE JOURNAL OF PHYSICAL CHEMISTRY A · JANUARY 2003

Impact Factor: 2.69 · DOI: 10.1021/jp021348e

CITATIONS

5

READS

173

4 AUTHORS, INCLUDING:



Jacek Zielonka

Medical College of Wisconsin

112 PUBLICATIONS 1,903 CITATIONS

SEE PROFILE

Benzopinacol Radical Cation

Jacek Rogowski, Jacek Zielonka, Andrzej Marcinek,* and Jerzy Gębicki

Institute of Applied Radiation Chemistry, Technical University, 90-924 Lodz, Poland

Paweł Bednarek

Department of Chemistry, University of Fribourg, Perolles, CH-1700 Fribourg, Switzerland

Received: June 5, 2002; In Final Form: July 25, 2002

The absorption spectrum of the elusive benzopinacol radical cation is presented for the first time. This species could be characterized spectroscopically in an argon and organic matrixes. On the basis of experimental results and density functional calculations the structure of the benzopinacol radical cation has been identified as that of a stable complex between two interacting moieties.

1. Introduction

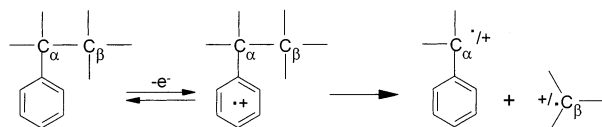
Organic radical ions undergo a rich variety of unimolecular and bimolecular reactions. Processes such as valence isomerization, rearrangement, and fragmentation are often significantly different from those of their neutral precursors.¹

Removal of an electron very often activates molecules for fragmentation, providing a useful method of breaking bonds that are quite strong in neutral substrates. This type of fragmentation is widely documented for radical cations by mass spectrometry. In the past decade there is also an enormous interest in the reactions in solution involving cleavage of σ bonds.² For example, such reactions have been intensively investigated from the practical point of view of degradation of lignine to lower and useful aromatics.³

For a large variety of aromatic compounds ionization and formation of a radical cation is followed by the cleavage of a side chain $C_\alpha-C_\beta$ bond.^{4,5} Among the groups on C_α and/or C_β which can favor the breaking of this bond, the OH group occupies a special position. It is known that compounds with OH groups such as 1- and 2-arylalkanols undergo very efficient bond cleavage reactions on oxidation (Scheme 1).⁶ From a mechanistic point of view, both the properties of the radical cation and the step involving the cleavage of the C–C bond, attract most attention.^{4,5} Despite the considerable amount of work carried out on this subject, relatively little information is available on the rate of the fragmentation process and the characterization of primary radical cations, especially in the case of benzopinacols. The unusually facile cleavage of benzopinacols requires the use of fast time-resolved spectroscopic methods to identify the reactive intermediates and the cleavage rates. However, even such unique techniques may not allow the direct characterization of the primary radical cation and even the rate of the process cannot be monitored directly, since pinacol radical cations have lifetimes < 10 ps.^{7,8}

Although Bockman et al.⁸ succeeded in measuring the ultrafast (10^{10} to 10^{11} s⁻¹) cleavage rates of benzopinacol radical cations, the spectroscopic characterization of these group of radical cations remains only fragmentary. The very elusive radical cation of benzopinacol, the model compound of the

SCHEME 1



series, has not been identified directly and no information on its structure is available. Therefore we have used the matrix isolation technique in frozen rare gas matrixes and organic glassy matrixes to achieve a full spectral and structural characterization of the primary product of ionization of benzopinacol. Moreover we will show that the properties of the benzopinacol radical cation have a profound influence on the following fragmentation process.

2. Results and Discussion

In matrixes, radical ions can be produced under stable conditions allowing their spectroscopic (UV–Vis, IR, ESR) characterization. Second, in rigid matrixes the lifetime of molecular ions increases due to suppression of diffusion-controlled recombination processes and the inhibitory effects of the matrix on fragmentation reactions. The low temperature also allows for monitoring of low barrier processes on a much longer time scale. There are two major methods of generation of radical cations in rigid matrixes: photolysis and radiolysis. A more generally applicable approach is the radiolytic method. The positive charges formed on the solvent molecules are transferred to substrate molecules of lower ionization potential. The combination of matrix isolation techniques with pulse radiolysis enables the direct measurement of kinetics for the investigated processes.^{1,9}

The inhibitory effect of the matrix on fragmentation processes can be demonstrated with the 10-methylacridine dimer (10,10'-dimethyl-9,9',10,10'-tetrahydro-9,9'-bisacridine). Under matrix conditions the dimer radical cation is stable and can be spectroscopically characterized. However, on thermal relaxation of the matrix to 90 K (slightly above the glassy transition temperature) the dimer radical cation dissociated to form the closed shell cation and the radical. The dissociation reaction takes place abruptly and the stabilization of the dimer radical cation is mostly due to the rigidity of the matrix at 77 K.¹⁰

* Author to whom correspondence should be addressed. E-mail: marcinek@ck-sg.p.lodz.pl.

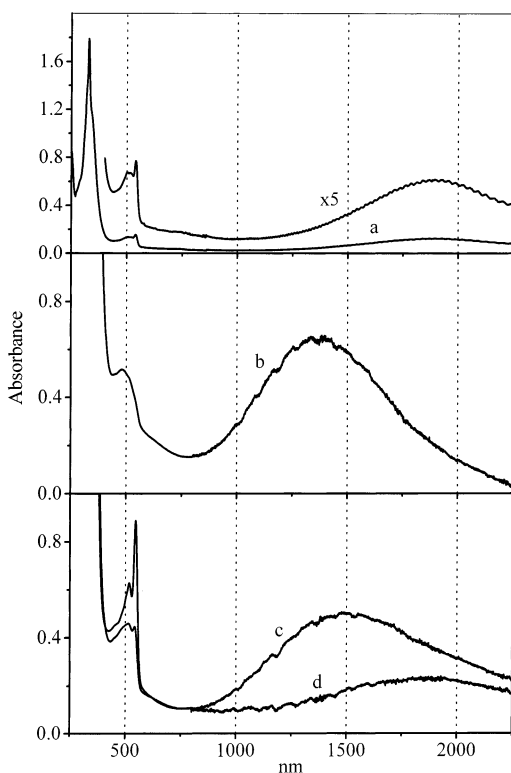
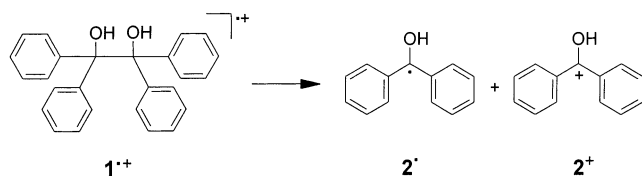


Figure 1. Electronic absorption spectrum (a) obtained after X-irradiation of an argon matrix containing benzopinacol, **1**. Spectrum (b) obtained after electron impact ionization of benzopinacol in 2-chlorobutane at 20 K (1×10^{-2} M solution, radiation dose 30 kGy, sample thickness 2 mm). Spectra (c) and (d) obtained after sample annealing at 60 (c) and 90 K (d) for 15 min.

SCHEME 2



X-irradiation of benzopinacol embedded in an argon matrix at 19 K results X-irradiation in the spectrum presented in Figure 1 (spectrum a). Three bands clearly dominate: a very strong narrow band located around 330 nm, a much weaker one around 500–550 nm, and a very broad band with $\lambda_{\text{max}} \approx 1900$ nm. Photolysis of the sample with near-IR light (> 900 nm) causes bleaching of all three bands, but this process is not very efficient and the observed effect can be attributed to the local heating on illumination. The band sequence around 500–550 nm in Figure 1a shows a pattern very characteristic for the diphenylhydroxymethyl radical (**2**[•]),^{9,11} although the photolysis experiments indicate also the participation of a second component in this band. The presence of product directly after ionization under cryogenic conditions is not surprising, as to some extent the fragmentation can be driven by the excess energy released in the highly exothermic charge transfer from Ar to **1**.¹ Also, the strongest band at 330 nm may be assigned to either or both fragmentation products, the diphenylhydroxymethyl radical (**2**[•]),^{9,11} and the closed shell cation (**2**⁺).¹² Therefore only the broad NIR band, not identified previously, can be unambiguously assigned to the primary radical cation **1**^{•+}. Much less excess energy is available after radiolytic ionization in organic glassy matrixes. In addition, this energy is more readily dissipated and hence not available to drive activated processes.¹ The spectrum obtained on radiolysis of benzopinacol embedded

in a 2-chlorobutane matrix at 20 K is presented in Figure 1b. The structureless absorption band at 480 nm does not resemble that of the diphenylhydroxymethyl radical **2**[•], which indicates that fragmentation has not taken place under these conditions. The absorption bands of the primary radical cation dominate in the spectrum. The strong band around 330 nm (not shown on the presented scale) is still present as in the spectrum measured in an argon matrix. An absorption band in this spectral region is characteristic for all transient species presented in this paper.

The major difference between the spectra obtained in argon compared to organic matrixes lies in the position of the long wavelength band. In 2-chlorobutane the maximum is at 1370 nm, which implies a 500 nm blue shift (< 0.3 eV). However, there is a close link between the two spectra. On annealing of the organic matrix, the maximum of the near-IR band shifts toward longer wavelengths and finally at 90 K it is almost identical to that observed in argon matrix (see Figure 1c,d). This shift is accompanied by a partial decay of the NIR band, especially at higher temperatures where fragmentation is no longer inhibited by matrix rigidity. A concomitant growth of the band at 545 nm, with its distinct structure characteristic of the diphenylhydroxymethyl radical,^{9,11} is observed. The thermal changes can be stopped, although not reversed, at any moment by freezing the matrix back to 20 K.

It is very likely that the shift observed in the radical cation spectrum is due to relaxation of the molecule geometry upon softening of the matrix. Such an influence of the matrix on the structure of a radical cation is often observed for large organic molecules which undergo significant structural relaxation on ionization.¹³ The potential energy surface for relaxation can be very flat and hence susceptible to distortion by cage effects. In organic glasses, the radical cation is probably frozen in a different form than that observed in argon matrix.

To achieve an unambiguous assignment of the observed absorption bands we carried out density functional calculations with the B3LYP combination of hybrid exchange and correlation functionals, modeling the one-electron density using the 6-31G* basis set.^{14–16} Geometry optimizations of neutral benzopinacol revealed an equilibrium structure of C_2 symmetry which does not, however, represent the global energy minimum. Extensive conformational searches using semiempirical procedures indicated several minima of C_1 symmetry. The lowest of these was reoptimized by B3LYP and found to lie 2.2 kcal/mol below the C_2 minimum. When an electron was removed from either structure, the resulting radical cations relaxed to geometries that differed only little from those of the parent neutral compound. The reason for this is that the orbital from which the electron is removed is centered on (and spread rather evenly over) the phenyl rings. These structures were found to be minima, i.e., they do not fragment spontaneously. Again, the C_1 minimum was found to lie below the C_2 minimum by 2.4 kcal/mol.

On stretching the central C–C bond to 1.8–1.9 Å, one arrives at a point where the SOMO (singly occupied molecular orbital) changes in nature and becomes centered on this bond which, according to theoretical predictions, is a prerequisite for the facile cleavage of the carbon–carbon bond.⁵ Once this point is reached, geometry optimization leads to spontaneous dissociation which leads, however, not to separated fragments, but to a species that must be regarded as a complex between a diphenylhydroxymethyl radical and the corresponding cation. In this process the central bond is elongated to 3.5 Å and the energy decreases by 31 kcal/mol, but the resulting species is still bound by 14.8 kcal/mol relative to the separated (and separately optimized) fragments. This seems to be a very reasonable

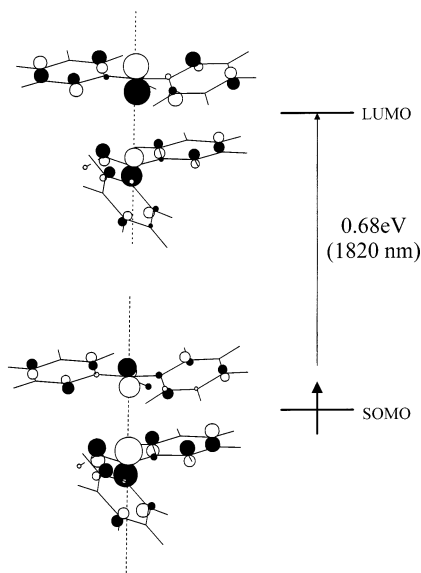
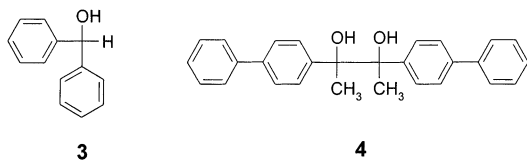


Figure 2. Molecular orbitals of the benzopinacol radical cation involved in the excitation corresponding to the near-IR absorption band. The areas of the spheres are proportional to the AO coefficients.

estimate for the binding energy of the complex since similar complexation enthalpy was found for aromatic dimer radical cations.^{1,17} As in case of the parent radical cation, a C_1 structure lies 2.4 kcal/mol below C_2 -symmetric structure which is attained if one starts from the C_2 neutral precursor.

According to B3LYP, about 62% of the spin resides in one-half and 60% of the charge in the other half of the complex. In view of the known tendency of density functional methods to overstabilize radical cations with a symmetric distribution of spin and charge relative to structures where the distribution is unsymmetric, the above finding is somewhat surprising.¹⁸ However, the fact that partial localization is predicted to be energetically favorable even by B3LYP indicates that there must be a strong driving force for this to occur.

To predict the electronic absorption spectrum of this complex, we carried out density-functional calculations based on time-dependent (TD) response theory as implemented in the Gaussian 98 program.^{16,19,20} We have previously applied this method successfully to open-shell systems of NADH analogues.²¹ According to TD-B3LYP/6-31G*, the complex radical cation should show a transition that corresponds to promotion of the unpaired electron from the bonding combination of fragment MOs (the former σ (C–C) orbital) to the antibonding combination (the former σ^* (C–C) orbital, cf. Figure 2) which is predicted to occur at 1820 nm, in excellent agreement with experiment. The position of this electronic transition will depend very much on the distance between the central carbon atoms, which could explain the shift of this band observed on annealing of the matrix.



TD-B3LYP/6-31G* predicts also two weaker absorption bands at 463 and 453 nm, which correspond predominantly to $\text{SOMO} \rightarrow \text{LUMO} + 1$ and $\text{SOMO} \rightarrow \text{LUMO} + 2$ electron promotion. The method predicts the position of these excited states in close proximity to the experimentally observed

TABLE 1: Comparison of the Experimentally Observed Absorption Bands of the Transient Species Generated from Benzopinacol to the Electronic Transitions Predicted by the TD-B3LYP/6-31G* Method (only electronic transitions with oscillator strength > 0.01 are presented)

	EAS nm	TD-B3LYP/ 6-31G* nm (f^a)	electronic transition ^b
radical-cation 1^{++}	1900	1820 (0.076)	72% $\text{SOMO} \rightarrow \text{LUMO}$
	480	463 (0.019)	69% $\text{SOMO} \rightarrow \text{LUMO}+1$
		453 (0.015)	77% $\text{SOMO} \rightarrow \text{LUMO}+2$
	330	352 (0.060)	75% $\text{HOMO}-1 \rightarrow \text{SOMO}$
		332 (0.257)	70% $\text{HOMO}-7 \rightarrow \text{SOMO}$
		330 (0.034)	79% $\text{HOMO}-2 \rightarrow \text{LUMO}$
		323 (0.358)	70% $\text{HOMO}-1 \rightarrow \text{LUMO}$
radical 2^+	332, 545 ^c		
	336, 560 ^d		
cation 2^+	346 ^e		
unfragmented		2022 (0.017)	63% $\text{HOMO}-3 \rightarrow \text{SOMO}$
radical-cation		1183 (0.057)	75% $\text{HOMO}-7 \rightarrow \text{SOMO}$
		1036 (0.072)	75% $\text{HOMO}-6 \rightarrow \text{SOMO}$
		829 (0.024)	94% $\text{HOMO}-8 \rightarrow \text{SOMO}$
		565 (0.015)	99% $\text{HOMO}-9 \rightarrow \text{SOMO}$
		310–480 (vw)	

^a Oscillator strength for electronic transition. ^b Dominant electron promotion. ^c Ref 11. ^d Ref 9. ^e Ref 12.

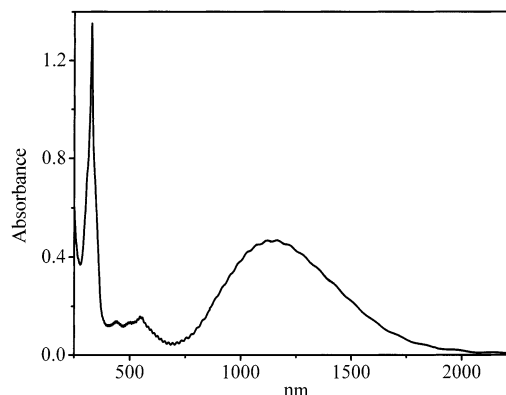


Figure 3. Electronic absorption spectra obtained after X-irradiation of an argon matrix containing diphenylmethanol.

structureless absorption band at around 480 nm. Also the series of transitions predicted below 350 nm (see Table 1) with two very strong absorptions at 332 and 323 nm fits the experimentally observed band at 330 nm.

We also carried out TD-B3LYP calculations for the unfragmented radical cation of benzopinacol (see above). According to those calculations the transitions for this species should differ significantly from the observed pattern of absorption bands and are rather reminiscent of the absorption of diphenylmethanol radical cation (3^{++}) with strong bands around 1100 nm (see Figure 3). This radical cation may thus serve as a model for the unfragmented benzopinacol radical cation. Although 3^{++} deprotonates to form also the diphenylhydroxymethyl radical 2^+ , this process takes place at higher temperatures only after softening of the matrix and is insignificant below 77 K.

Although the absorption of the relaxed radical cation 1^{++} observed in an argon matrix is different from that predicted for the unfragmented species, the absorption bands observed in organic glassy matrixes at 20 K are much closer to that pattern. Whether the frozen structure of the radical cation in organic glasses belongs to the unfragmented species, or whether the cleavage has already taken place, cannot be easily distinguished. However, as the changes observed on annealing are very smooth and can be frozen at any moment, we prefer to assign them to the relaxation of the complex radical cation rather than to the

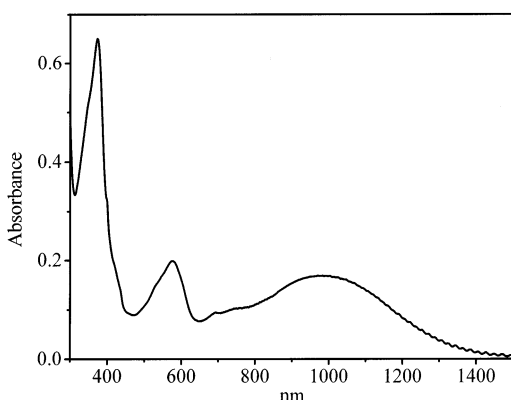


Figure 4. Electronic absorption spectra obtained after X-irradiation of an argon matrix containing 2,3-bis-(4'-biphenyl)2,3-butanediol.

actual cleavage process. Therefore, we believe that at 20 K benzopinacol radical cation has already dissociated to the extent limited only by the rigid cage in which it is enclosed under these conditions. The following changes observed in the spectra in slow motion reflect the process of separation of the fragments, and the formation of the most stable conformation of the complex. Matrix cage effect does not protect the primary radical cation against fragmentation even at very low temperatures, and the activation barrier for this process must be extremely low. The radical cation achieves stronger stabilization only in the form of the complex.

Interestingly, TD-B3LYP/6-31G* does not predict any strong absorption bands between 310 and 500 nm for the unfragmented species. Therefore, the presence of the strong band at 330 nm in the spectrum measured in the organic glass gives additional support for assignment of that spectrum to the complex radical cation.

Above, we have presented the first spectroscopic and structural characterization of the radical cation of benzopinacol. Its very weak absorption in the visible region explains why this radical cation, the parent compound of the benzopinacole series, could not previously be characterized by femtosecond flash photolysis methods.⁸ However, much more beneficial was the investigation of 2,3-bis-(4'-biphenyl)2,3-butanediol (**4**), which was found to absorb already at 730 nm. This absorption was assigned to the radical cation of **4** based on its occurrence in the spectrum of the radical cation of methylbiphenyl which was thought to be the chromophore responsible for the absorption of **4**^{+,8}

The spectrum of the radical cation **4**⁺ in an Ar matrix, presented in Figure 4, is characterized by three strong absorption bands at 375, 575, and 990 nm. The first two bands might, however, represent a superposition of the absorptions of the primary radical cation and that of the fragmentation products formed in the course of ionization.¹¹ Indeed, illumination of the sample (>810 nm) indicates the presence of at least two components in the bands at 375 and 545 nm. Poor solubility of this compound in organic glassy matrixes limits the possibility of an analysis such as that presented above for the benzopinacol radical cation. However, the assignment of the broad band around 1000 nm to the radical cation seems to be unambiguous and is in agreement with the results of Bockman et al. if one assumes that these authors were able to monitor only the part of this absorption band.⁸

3. Conclusions

We have presented for the first time the absorption spectrum of the very elusive radical cation of benzopinacol, **1**⁺, which

was assigned with the help of time-dependent density functional calculations. B3LYP/6-31G* predicts that **1**⁺ is stabilized in a form of a complex consisting of two interacting diphenylhydroxymethyl moieties. The near-IR absorption band of **1**⁺ is ascribed to a $\sigma \rightarrow \sigma^*$ electronic transition between the C–C bonding and antibonding combination of molecular orbitals which are mainly located on the benzylic carbon atoms of both fragments. The shift of this band which occurs on matrix relaxation is thought to reflect the process of separation of the two fragments and the formation of the equilibrium conformation of the complex. The very weak absorption of **1**⁺ in the visible region explains the failure of its characterization in previous laser flash photolysis experiments. In contrast, the blue-shifted near-IR absorption band in the case of the 2,3-bis-(4'-biphenyl)2,3-butanediol radical cation allowed confirmation of the previous identification of this elusive species.

4. Experimental Section

4.1. Materials. All chemicals were purchased from Aldrich and were purified by standard laboratory procedures as necessary except 2,3-bis-(4'-biphenyl)2,3-butanediol which was synthesized according to described procedure.⁸

4.2. Matrix Isolation and Spectroscopy. Crystals of the compounds were placed in a U-shaped tube immersed in a water bath and connected to the inlet system of a closed-cycle cryostat. A mixture of argon and methylene chloride flowing through the tube at a rate of ≈ 1 mmol/h swept the compounds onto a CsI window held at 19 K. There the mixture accumulated to form a matrix containing a sufficient quantity of the compound within 2 h. After taking reference spectra, the samples were exposed to 90 min of X-irradiation.

Glassy samples of 2-chlorobutane were prepared by quench-freezing of room temperature solutions in liquid nitrogen. The samples were 2 mm thick and were placed in a temperature-controlled, liquid helium-cooled cryostat (Oxford Instruments). The desired temperature of the matrix was attained by a flow of helium and automatically controlled heating. To achieve a fast equilibration of the sample temperature the glassy matrix was directly exposed to the helium flow by removing a side wall of the sample cell. A description of the pulse radiolysis system and methodology of the low-temperature studies in organic matrixes are given elsewhere.^{22,23}

The optical absorption spectra were measured on a Cary 5 spectrophotometer (Varian).

4.3. Quantum Chemical Calculations. The geometries of all species were optimized by the B3LYP density functional method¹⁴ as implemented in the Gaussian 98 suite of programs,¹⁶ using the 6-31G* basis set. Relative energies were calculated at the same level. Full sets of Cartesian coordinates and absolute energies are given in the Supporting Information.

Electronic transitions were predicted by density functional-based time-dependent response (TDR) theory.¹⁹ We used the formulation of TD-DFT described by Stratmann et al.²⁰ and implemented in the Gaussian 98 program,¹⁶ together with the B3LYP functional and the 6-31G* basis set.

Acknowledgment. This work was supported by a grant from the State Committee for Scientific Research (No. 3/T09A/037/17). We thank Prof. John Penn (West Virginia University at Morgantown) for participation in early stages of this project and Prof. Thomas Bally (University of Fribourg, Switzerland) for discussion.

Supporting Information Available: Listing of Cartesian coordinates from the B3LYP calculations as well as energies

for transient species mentioned in this study are available in ASCII format. This material is available free of charge via the Internet at <http://pubs.acs.org>.

References and Notes

- (1) (a) Gębicki, J.; Marcinek, A. In *General Aspects of the Chemistry of Radicals*; Alfassi, Z. B., Ed.; Wiley: Chichester, 1999; p 175. (b) Bally, T. In *Radical Ionic Systems*; Lund, A., Shiotani, M., Eds.; Kluwer: Dordrecht, 1991; p 3.
- (2) (a) Chanon, M.; Rajzmann, M.; Chanon, F. *Tetrahedron* **1990**, *46*, 6193. (b) Maslak, P. *Top. Curr. Chem.* **1993**, *168*, 1. (c) Savéant, J.-M. *Tetrahedron* **1994**, *50*, 10117.
- (3) (a) Pardini, V. L.; Smith, C. Z.; Utley, J. H. P.; Vargas, R. R.; Viertler, H. *J. Org. Chem.* **1991**, *56*, 7305. (b) Labat, G.; Meunier, B. *J. Org. Chem.* **1989**, *54*, 5008. (c) Habe, T.; Shimada, M.; Okamoto, T.; Panijpan, B.; Higuchi, T. *J. Chem. Soc., Chem. Commun.* **1985**, 1323. (d) Haenel, M. W.; Richter, U.-B.; Solar, S.; Getoff, N. *Z. Naturforsch.* **1995**, *50b*, 303.
- (4) (a) Maslak, P.; Chapman, W. H.; Vallombroso, T. M.; Watson, B. A. *J. Am. Chem. Soc.* **1995**, *117*, 12380. (b) Okamoto, A.; Snow, M. S.; Arnold, D. R. *Tetrahedron* **1986**, *42*, 6175. (c) Reichel, L. W.; Griffin, G. W.; Muller, J.; Das, P. K.; Ege, S. N. *Can. J. Chem.* **1984**, *62*, 424. (d) Gaillard, E. R.; Whitten, D. G. *Acc. Chem. Res.* **1996**, *29*, 292. (e) *Photoinduced Electron Transfer, Part C*; Fox, M. A., Chanon, M., Eds.; Elsevier: Amsterdam, 1988. (f) Faria, J. L.; McClelland, R. A.; Steenken, S. *Chem. Eur. J.* **1998**, *4*, 1275.
- (5) (a) Baciocchi, E.; Bietti, M.; Lanzalunga, O. *Acc. Chem. Res.* **2000**, *33*, 243. (b) Popielarz, R.; Arnold, D. R. *J. Am. Chem. Soc.* **1990**, *112*, 3068.
- (6) (a) Penn, J. H.; Duncan, J. H. *J. Org. Chem.* **1993**, *58*, 2003. (b) Han, D. S.; Shine, H. J. *J. Org. Chem.* **1996**, *61*, 3977. (c) Davis, H. F.; Das, P. K.; Reichel, L. W.; Griffin, G. W. *J. Am. Chem. Soc.* **1984**, *106*, 6968. (d) Albin, A.; Spreti, S. *J. Chem. Soc., Perkin Trans. 2* **1987**, 1175.
- (7) Sankararaman, S.; Kochi, J. K. *J. Chem. Soc., Perkin Trans. 2* **1993**, 825.
- (8) Bockman, T. M.; Hubig, S. M.; Kochi, J. K. *J. Am. Chem. Soc.* **1998**, *120*, 6542.
- (9) Shida, T. *Electronic absorption spectra of radical ions*; Elsevier: Amsterdam, 1988.
- (10) Adamus, J.; Rogowski, J.; Michalak, J.; Paneth, P.; Gębicki, J.; Marcinek, A.; Platz, M. S. *J. Phys. Org. Chem.* **1993**, *6*, 254.
- (11) Hayon, E.; Ibata, T.; Lichtin, N. N.; Simic, M. *J. Phys. Chem.* **1972**, *76*, 2072.
- (12) Ireland, J. F.; Wyatt, P. A. H. *J. Chem. Soc., Perkin Trans. 1* **1973**, *69*, 161.
- (13) (a) Marcinek, A.; Rogowski, J.; Adamus, J.; Gębicki, J.; Platz, M. S. *J. Phys. Chem.* **1996**, *100*, 13539. (b) Marcinek, A.; Zielonka, J.; Adamus, J.; Gębicki, J.; Platz, M. S. *J. Phys. Chem. A* **2001**, *105*, 875.
- (14) (a) Becke, A. D. *J. Chem. Phys.* **1993**, *98*, 5648. (b) Lee, C.; Yang, W.; Parr, R. G. *Phys. Rev. B* **1988**, *37*, 785.
- (15) Johnson, B. G.; Gill, P. M. W.; Pople, J. A. *J. Chem. Phys.* **1993**, *98*, 5612.
- (16) Frisch, M. J.; Trucks, G. W.; Schlegel, H. B.; Scuseria, G. E.; Robb, M. A.; Cheeseman, J. R.; Zakrzewski, V. G.; Montgomery, J. A.; Stratmann, R. E.; Burant, J. C.; Dapprich, S.; Millam, J. M.; Daniels, A. D.; Kudin, K. N.; Strain, M. C.; Farkas, O.; Tomasi, J.; Barone, V.; Cossi, M.; Cammi, R.; Mennucci, B.; Pommelli, C.; Adamo, C.; Clifford, S.; Ochterski, J.; Petersson, G. A.; Ayala, P. Y.; Cui, Q.; Morokuma, K.; Malick, D. K.; Rabuck, A. D.; Raghavachari, K.; Foresman, J. B.; Cioslowski, J.; Ortiz, J. V.; Stefanov, B. B.; Liu, G.; Liashenko, A.; Piskorz, P.; Komaromi, I.; Gomperts, R.; Martin, R. L.; Fox, D. J.; Keith, T.; Al-Laham, M. A.; Peng, C. Y.; Nanayakkara, A.; Challacombe, M.; Gill, P. M. W.; Johnson, B. G.; Chen, W.; Wong, M. W.; Andres, J. L.; Gonzales, C.; Head-Gordon, M.; Repogle, E. S.; Pople, J. A. *Gaussian 98*, revision A.1; Gaussian, Inc.: Pittsburgh, PA, 1998.
- (17) (a) Badger, B.; Brocklehurst, B. *Trans. Faraday Soc.* **1965**, *65*, 2576, 2588. (b) Badger, B.; Brocklehurst, B. *Trans. Faraday Soc.* **1966**, *66*, 2939. (c) El-Shall, M. S.; Meot-Ner (Mautner), M. *J. Phys. Chem.* **1987**, *91*, 1088.
- (18) Bally, T.; Sastry, G. N. *J. Phys. Chem. A* **1997**, *101*, 7923.
- (19) Casida, M. E. In *Recent Advances in Density Functional Methods, part I*; Chong, D. P., Ed.; World Scientific: Singapore, 1995; p 155.
- (20) Stratmann, R. E.; Scuseria, G. E.; Frisch, M. J. *J. Chem. Phys.* **1998**, *109*, 8218.
- (21) (a) Marcinek, A.; Adamus, J.; Huben, K.; Gębicki, J.; Bartczak, T.; Bednarek, P.; Bally, T. *J. Am. Chem. Soc.* **2000**, *122*, 437. (b) Marcinek, A.; Adamus, J.; Gębicki, J.; Platz, M. S.; Bednarek, P. *J. Phys. Chem. A* **2000**, *104*, 724.
- (22) Karolczak, S.; Hodyr, K.; Łubis, R.; Kroh, J. *J. Radioanal. Nucl. Chem.* **1986**, *101*, 177.
- (23) Gębicki, J.; Marcinek, A.; Rogowski, J. *J. Radiat. Phys. Chem.* **1992**, *39*, 41.